



CrossMark  
click for updates

Cite this: *RSC Adv.*, 2016, 6, 5575

# Chitosan containing azo-based Schiff bases: thermal, antibacterial and birefringence properties for bio-optical devices†

Nidhi Nigam,<sup>a</sup> Santosh Kumar,<sup>†a</sup> P. K. Dutta,<sup>\*a</sup> S. Pei<sup>b</sup> and Tamal Ghosh<sup>\*a</sup>

The present investigation describes the preparation of chitosan/2-hydroxy-5-(4-nitrophenylazo)-benzaldehyde (CHNAB) and chitosan/2-hydroxy-5-(4-tolylazo)-benzaldehyde (CHMAB) derivatives (in 4 : 5 molar ratio) under mild conditions. These derivatives were synthesized by 79% and  $\leq 90\%$  deacetylated chitosan in an isopropyl alcohol/water mixture and dimethyl sulfoxide. The thermal properties of the derivatives were examined by differential scanning calorimetry (DSC) and thermogravimetric analysis (TGA). CHNAB shows an endothermic peak at 212 °C and exothermic peak at 231 °C due to phase change for *cis*–*trans* isomerisation, whereas, in CHMAB, only the endothermic peak at 222 °C is seen due to the absence of *cis*–*trans* isomerisation. Toxicity has been reduced in chitosan based azo derivatives, as compared to the corresponding azo compounds, as seen by the antibacterial results where *S. aureus* (Gram positive) shows ZOI 26 mm for CHNAB and 38 mm for CHMAB. The transmitted signal intensity induced by the birefringence as shown by CHNAB as  $\pi d\Delta n/\lambda$  is much less than 1. The transmitted signal is effectively proportional to  $(\Delta n)^2$  because of the nitro group behaving like an auxochrome. The study on the optical birefringence properties of the azo-based chitosan derivatives indicates that the prepared derivatives may be used as bio-optical devices for biomedical applications.

Received 19th December 2015  
Accepted 2nd January 2016

DOI: 10.1039/c5ra27210f

www.rsc.org/advances

## Introduction

Polymer based azo materials have attracted huge attention in the past few decades due to their enormous potential applications in optical information transmission, optical data storage, optical switching, nonlinear optical (NLO) materials.<sup>1–6</sup> Polymeric nonlinear optical (NLO) materials have been widely used for lower switching voltage and higher band width electro-optic devices and have become a subject area of intense research interest in recent years. Properties such as high electro-optic constant and low dielectric constant have made the NLO polymers more advantageous which has been extensively demonstrated by different research groups.<sup>7–11</sup> For polymeric based devices to effectively compete with inorganic materials, issues such as optical insertion loss and thermal stability have to be improved.

Chitosan possesses interesting characteristics, such as its ability to induce a minimal foreign body reaction, an intrinsic

antibacterial nature.<sup>12</sup> Chitosan in solution and gel forms exhibit strong antimicrobial activity against a broad spectrum of both Gram-positive and Gram-negative medically relevant microorganisms.<sup>13</sup> The antimicrobial nature of chitosan is due to surface–surface interactions between the biopolymer chains and microbial cell walls. Thus, chitosan based materials have the potential for antimicrobial action, the exploitation of which is of particular interest to the development of medical technologies. Azo dye containing polymers are studied with immense interest because of their unique photoinduced effects.<sup>14,15</sup> The photoisomerization process, which implies mobility of the azo dye molecules, results in a facile change in its orientation due to the polarized optical field and has been observed even in high glass transition polymer matrices.

In the present paper, we have described the preparation of chitosan/2-hydroxy-5-(4-nitrophenylazo)-benzaldehyde (CHNAB) and chitosan/2-hydroxy-5-(4-tolylazo)-benzaldehyde (CHMAB) derivatives using 79% and  $\leq 90\%$  deacetylated chitosan in isopropyl alcohol/water mixture and dimethyl sulfoxide under mild conditions. The thermal property of the derivatives has been investigated by differential scanning calorimetry (DSC) and thermogravimetric analysis (TGA). The methyl group containing derivative CHMAB shows wide spectrum antimicrobial activity against *S. aureus* which is much higher compared to free chitosan. Chitosan derivatives, both having azobenzene chromophore attached to chitosan polymer systems, display photoinduced birefringence in the form of solid films.

<sup>a</sup>Department of Chemistry, Motilal Nehru National Institute of Technology, Allahabad – 211004, India. E-mail: pkd@mnnit.ac.in; tamalghosh@mnnit.ac.in; Fax: +91 532 2545341

<sup>b</sup>Department of Physics, Jilin University, P. R. China

† Electronic supplementary information (ESI) available. See DOI: 10.1039/c5ra27210f

‡ Present address: Department of Chemistry, University of Coimbra, Coimbra, Portugal.

## Experimental methods

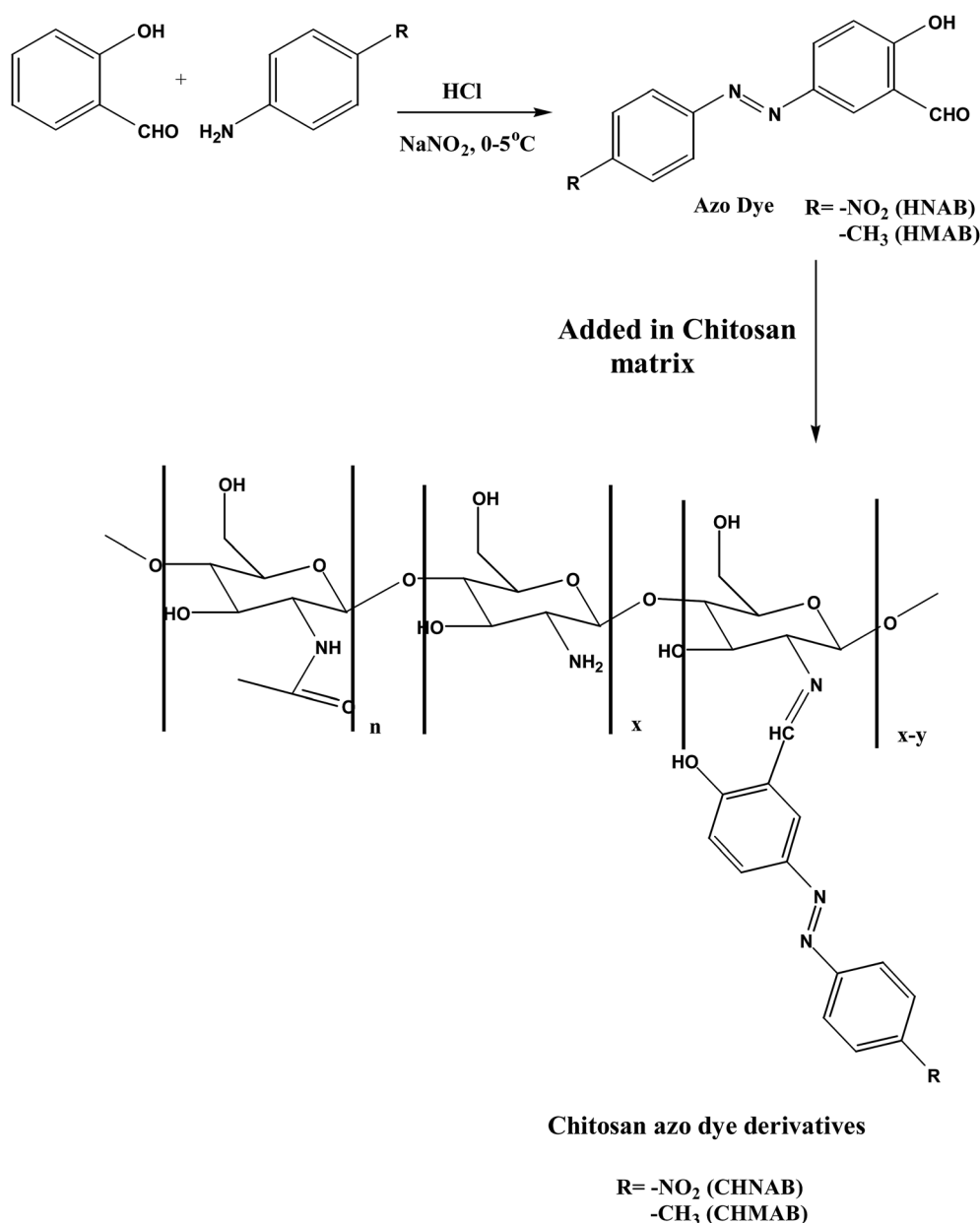
### Preparation of chitosan azo dye derivatives

2-Hydroxy-5-(4-nitrophenylazo)-benzaldehyde/2-hydroxy-5-(4-tolylazo)-benzaldehyde was dissolved in 5 mL of isopropyl alcohol and 1 mL of water was added to raise the dielectric constant of the isopropyl alcohol more than 40% of the solution. 50 mg of chitosan powder was immersed into the acetic acid solution at pH 4 (maintaining 4 : 5 molar ratio for chitosan : azo dye) and slowly stirred at room temperature for half an hour and the swollen mixture was kept in 0 °C for 3 days. The obtained product was successively washed with an isopropyl alcohol and water mixture (5 : 1, v/v) and dried in air (Scheme 1). The product was re-crystallized from *N,N*-dimethylacetamide

(DMAc) and isopropyl alcohol solution and washed several times with isopropyl alcohol/water mix-solvent. The final product was dried and kept in desiccators for further studies.

### Characterization of the azo based chitosan derivatives CHNAB and CHMAB

The azo dyes 2-hydroxy-5-(4-nitrophenylazo)-benzaldehyde (HNAB) and 2-hydroxy-5-(4-tolylazo)-benzaldehyde (HMAB) were synthesized according to literature procedure.<sup>16</sup> The recrystallised azo dyes were finally added in chitosan matrix resulting in the formation of the corresponding Schiff bases. Chitosan derivative obtained from HNAB and HMAB is named as CHNAB and CHMAB respectively. The azo based chitosan derivatives were characterized by FTIR spectroscopy. The



Scheme 1 Preparation of chitosan derivatives CHNAB and CHMAB.

infrared spectra were recorded on Perkin Elmer RX1 FTIR spectrophotometer using KBr pallets. Thermogravimetric analysis (TGA) with Perkin Elmer diamond and differential scanning calorimetry (DSC) with Pyris-6 heating and cooling rates of 10 °C were used.

### Biological activity: antimicrobial assay

The antimicrobial activity of chitosan and chitosan containing azo based Schiff bases were carried out using agar plate diffusion method. In this method, the solution (1 mg mL<sup>-1</sup>) of the Schiff base was absorbed in sterilized discs (approximately 60 µL of solution) and the antimicrobial activity was evaluated against two different test cultures *viz.* Gram negative bacteria *E. coli* and Gram positive bacteria *S. aureus*. The sterilized discs were placed on nutrient agar plates making lawns of the above test cultures. The plates were then incubated at 37 °C for 24 h. The diameters of the inhibitory zone surrounding discs were then measured.

### Birefringence measurement

Birefringence in azo-polymer films may be created by *trans-cis-trans* photoisomerization processes produced with a linear polarized light, with the induced orientation of the chromophores being perpendicular to the polarization direction. The anisotropic molecular orientation results in stable photoinduced birefringence or dichroism which can be erased by randomization of the alignment with circularly polarized light or heat. The experimental setup for the measurement of the photoinduced birefringence is shown in Fig. 1. The 532 nm line from a Nd:YAG laser was used as a pump (or writing) beam, and the 632.8 nm line from a He-Ne laser was used as a probe (or reading) beam. To carry out the experiments, a film sample was placed between a pair of crossed polarizers. To achieve maximum signal, the polarization vector of the pump beam was set to 45° with respect to the polarization vector of the probe beam. When needed, a quarter-wave plate (not shown in the figure) was inserted into the optical path of the pump beam before the sample (the quarter-wave plate converted the linear polarized beam to circular polarization which removed the birefringence that had been induced). The power of the pump

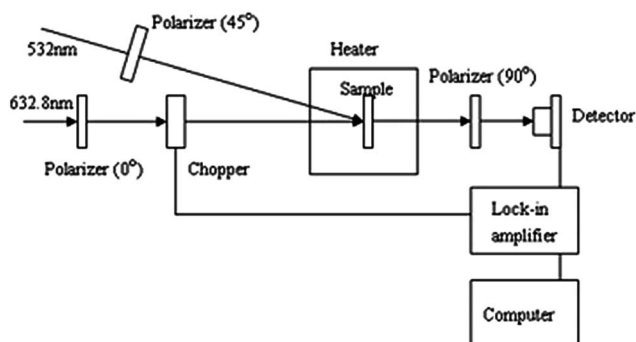


Fig. 1 Experimental setup for the measurement of optically induced birefringence.

laser was 23 mW and the diameter of the beam was approximately 0.3 cm.<sup>17,18</sup>

## Results and discussion

Preparation of chitosan/2-hydroxy-5-(4-nitrophenylazo)-benzaldehyde (CHNAB) and chitosan/2-hydroxy-5-(4-tolylazo)-benzaldehyde (CHMAB) derivatives (in 4 : 5 molar ratio) under mild conditions is shown in Scheme 1. We have synthesized two different derivatives CHNAB and CHMAB to explore the effect of electron-withdrawing (NO<sub>2</sub>) and electron-donating (CH<sub>3</sub>) group, respectively in thermal, antibacterial and birefringence properties.

### Differential scanning calorimetry analysis

DSC curves of chitosan derivatives recorded in nitrogen from 10 °C temperature to 400 °C are shown in Fig. 2. The temperatures for various thermal effects are represented for the derivative CHNAB, the endothermic peaks at 91 °C due to the type and length of the side chains. Endothermic peak at 212 °C and exothermic peak at 231 °C is due to the phase change and simultaneously decomposition of derivative, in most of the

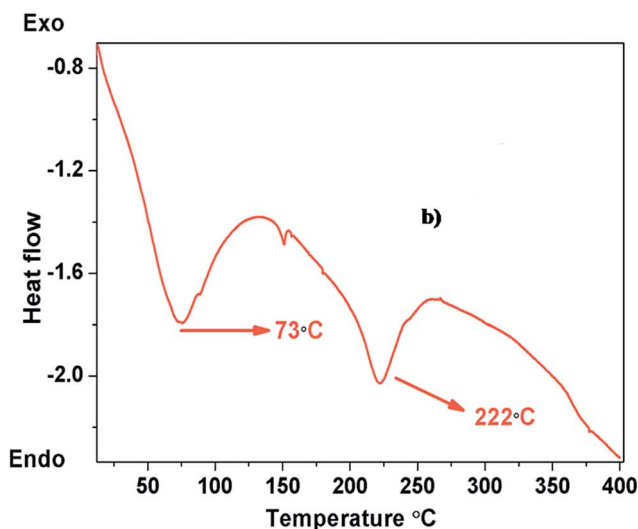
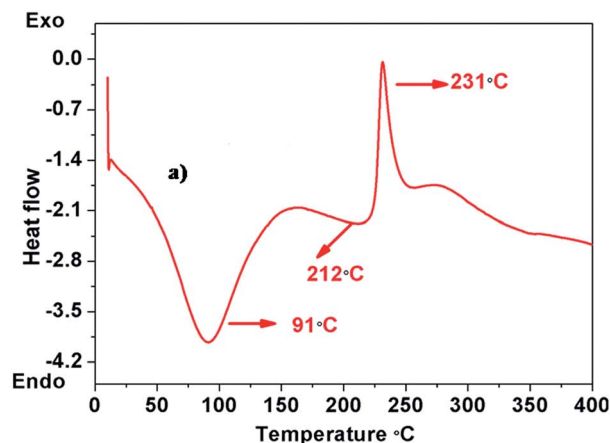


Fig. 2 DSC thermogram of (a) CHNAB and (b) CHMAB.

nitro group ( $-\text{NO}_2$ ) containing compounds such decomposition trends is observed.<sup>19</sup> In CHMAB, the endothermic peak at 73 °C is due to the presence of side chains, and peak at 222 °C is due to the phase change.

### Thermogravimetric and differential thermal analysis

Fig. 3 shows the thermogravimetric analysis of chitosan derivatives reveal the fact that the decomposition occurs in three consecutive steps. In case of CHNAB degradation of first step 4% loss by mass is in the temperature range of 60–94 °C. Due to the side chain groups present in derivative, second step 51% loss by mass in the temperature range 94–273 °C, due to acetyl and various hydrogen bonding functional groups present in the chitosan derivative. Third step 45% loss by mass in the temperature range 273–480 °C due to the loss of C=N and other moieties. No residual is left lastly, so the nitro derivative is less stable as compared to methyl one which can be justified by decomposition temperature ( $T_d$ ) = 227 °C and where as  $T_d$  for methyl derivative is  $T_d$  = 250 °C.

In case, of CHMAB the same first step 20% loss by mass in the temperature range of 60–260 °C due to the groups present in the chitosan derivative. Second step 27% loss by mass in temperature range 260–370 °C due to C=N and some groups. Third step 67.6% loss by mass in the range 370–650 °C and residual of 6.4% is left. This shows that methyl derivative is more stable as compared to nitro derivative which is also supported by DSC.

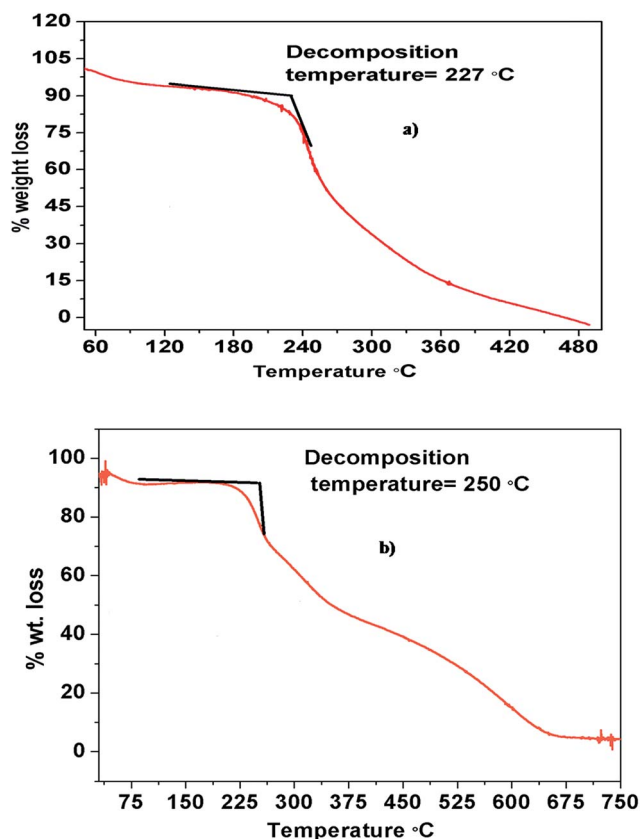


Fig. 3 TGA of (a) CHNAB and (b) CHMAB.

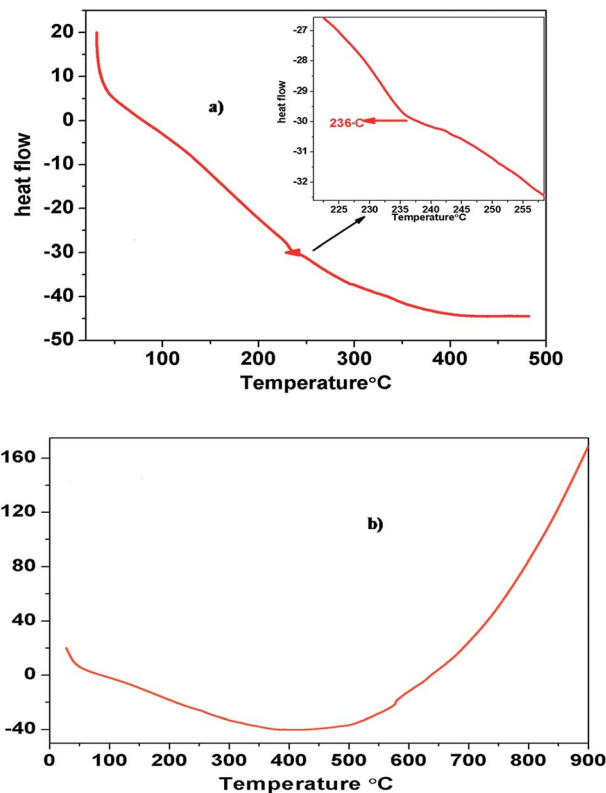


Fig. 4 DTA of (a) CHNAB and (b) CHMAB.

DTA of both derivatives shows the endothermic peaks showing the phase change which can be easily observed in Fig. 4.

### Antibacterial activity

Fig. 5 shows a typical antibacterial test result of chitosan as control in DMSO (A) and chitosan based Schiff bases (B and C)

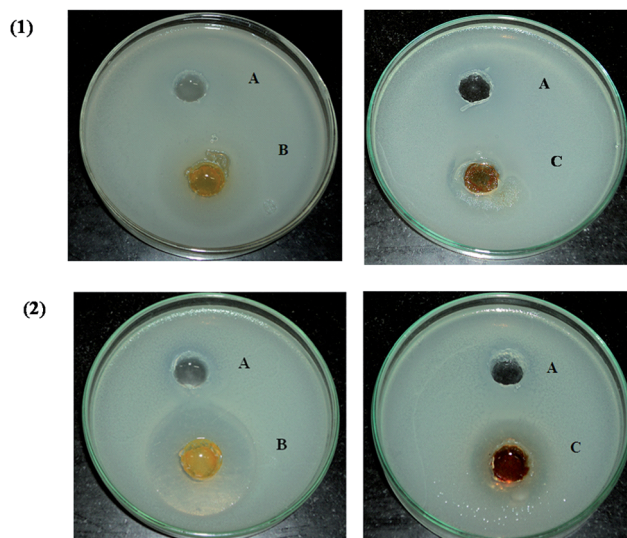


Fig. 5 Inhibitory effect of chitosan as control in DMSO (A), CHMAB (B) and CHNAB (C) against *E. coli* (1) and *S. aureus* (2).

**Table 1** Diameter of inhibitory zone of chitosan in DMSO as control and the Schiff bases against *E. coli* and *S. aureus*

Test culture	Diameter of inhibitory zone (mm)		
	Chitosan as control in DMSO (A)	CHMAB (B)	CHNAB (C)
<i>E. coli</i>	15	30	Nil
<i>S. aureus</i>	20	38	26

against *S. aureus* and *E. coli* as determined by the agar diffusion plate method. As shown in the figure, antibacterial activity, determined by the diameter of the growth inhibition zone, was dependent on the test sample used. The inhibition zone diameters (mm) of two samples were examined into two microorganisms, and the results are shown in Table 1. The agar diffusion test is a method commonly used to examine antimicrobial activity regarding the diffusion of the compound tested through water-containing agar plate.

The appearance and size of the clear zone in the disk method is mainly dependent on the ratio of disk area and size of inoculum, type of solid medium, and contact area. The surrounding clearing zone of CHMAB showed a very clear inhibitory zone of both Gram-positive and Gram-negative bacteria. It was generally caused by the maximum capability of chitosan polymer to carry active agents beside the occurrence of functional groups interaction phenomenon. The diffusion itself is dependent on the size, shape and polarity of the diffusing material. The antibacterial mechanism of chitosan is generally considered due to its positively charged amino group at the C-2 position of the glucosamine residue which interacts with negatively charged microbial cell membranes, leading to the leakage of proteinaceous and other intracellular constituents of the microorganisms.<sup>20</sup> The results revealed that chitosan azo derivative with a methyl group shows a very clear and greater inhibitory effect against *S. aureus* and *E. coli* in comparison to the derivative with the nitro group. The effect of the polymer complex on *E. coli* is not as effective as on *S. aureus*, which can be attributed to their different cell wall structures, the major constituent of its cell wall is peptidoglycan and there is very little protein.

### Birefringence studies

When illuminated with a polarized light of appropriate wavelength, the azobenzene groups undergo a reversible *trans-cis-trans* isomerisation process and an associated orientational redistribution of the chromophores. Appropriate substitution of the azobenzene chromophores may be used to tune the chromatic features from UV through the visible spectrum. The azo dye molecules are predominantly in the *trans*-state at room temperature and are isotropically distributed. When excited by a linearly polarized blue-green light (488 nm), preferential molecular excitation and the associated photoisomerization process results in an orientational hole burning. The orientational redistribution of the dye molecules with respect to the

polarization direction of the irradiating light finally leaves the *trans* isomers predominantly oriented perpendicular to this direction. Successive photoisomerization cycles result in a net dichroism and birefringence induced in the material due to the absorbance and refractive index difference in the parallel and perpendicular directions (to the incident polarization direction).

Fig. 6 shows the representative growth and decay traces of the birefringence signal. As the azo compound molecules are randomly oriented, no light is transmitted through the analyzer in the beginning of the experiment. As the pump laser radiation is introduced (point A in the figure), an anisotropic orientation distribution is created as a result of the accumulation of *cis* isomers and *trans* isomers that are oriented with the transition dipole vertical to the polarization vector of the pump beam. Light was, thus, transmitted through the analyzer because of the onset of birefringence. When the excitation light is turned off (point B in the figure), as shown in the figure, relaxation of the anisotropic steady state occurs.

However, the relaxation is not complete; parts of the induced birefringence are still held. To remove the remaining birefringence, circularly polarized light is introduced (point C in the

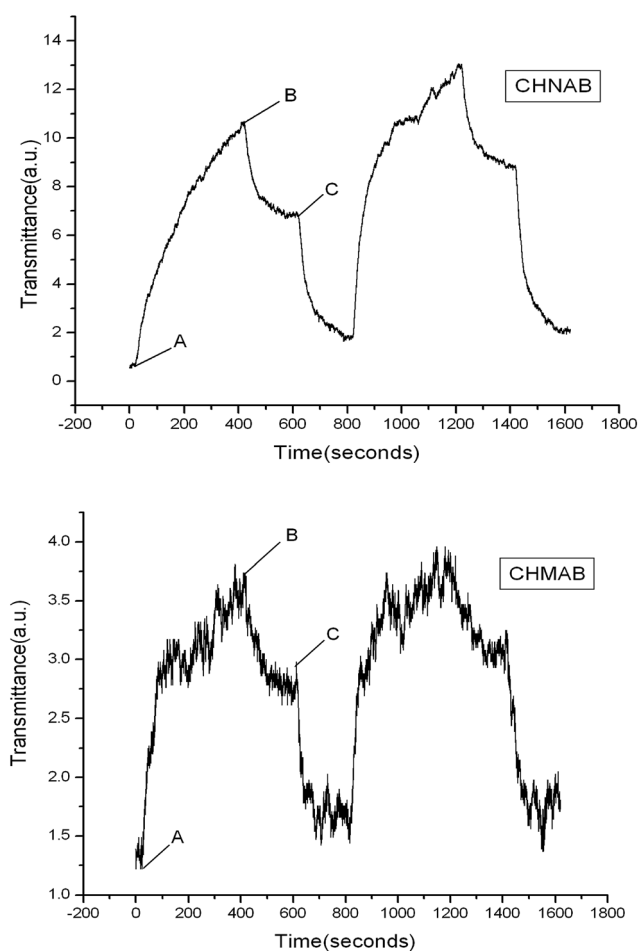


**Fig. 6** Experimental birefringence results of CHNAB and CHMAB at room temperature.

bottom figure). The circularly polarized light effectively converted the *cis* isomers to the *trans* form for all orientations. The transmitted signal intensity induced by the birefringence is proportional to  $\sin^2(\pi d \Delta n / \lambda)$ , where  $d$  is the thickness of the film,  $\Delta n$  is the birefringence of the film, and  $\lambda$  is the wavelength of the probe beam (632.8 nm).<sup>21,22</sup> Because  $\pi d \Delta n / \lambda$  is much less than 1, the transmitted signal is effectively proportional to  $(\Delta n)^2$ .<sup>23</sup> Birefringence is observed more in case of CHNAB as compared to the CHMAB because the derivative containing nitro group (CHNAB) shows more transmittance as compared to the methyl group derivative (CHMAB), as nitro group is acting like an auxochrome.

Two competing processes defined the maximum achievable birefringence: the orientation due to photoisomerization and the thermal relaxation that tended to disorientate the azobenzene groups. As the temperature increases, the second process becomes more important than the first one. These two competing processes are also likely to be relevant for the kinetics of the build up and decay of birefringence. The curves for the build up process can be well fitted with a biexponential function.<sup>23</sup>

The curves of build up and decay processes can be well fitted by using

$$y = A(1 - e^{-k_a t}) + B(1 - e^{-k_b t}) \quad (1)$$

where,  $A$  and  $B$  are pre exponential factors,  $t$  is the time, and  $k_a$  and  $k_b$  are the rate constants for writing the fast and slow processes, respectively. Actually,  $k_a$  has been shown to depend on the quantum yield of the isomerization reaction, the isomerization rate, and the local mobility of the azo dye, which are affected by the size of the azo moiety, the free volume around it, and the strength of the coupling interactions between the azo dye and the polymer backbone. The magnitude of  $k_b$  depends mainly on the polymer mobility. The curves for the decay could also be fitted with another biexponential function:

$$y = Ce^{-k_c t} + De^{-k_d t} + E \quad (2)$$

where  $C$  and  $D$  are the amplitudes associated with the processes having rate constants  $k_c$  and  $k_d$ , respectively and  $E$  is the background intensity, which can be minimized if, as mentioned above, the circular polarized light is introduced to erase the residual birefringence. The fast decay is due to the fast component of the thermal *cis-trans* isomerisation and dipole reorientation, whereas the slow decay is associated with the

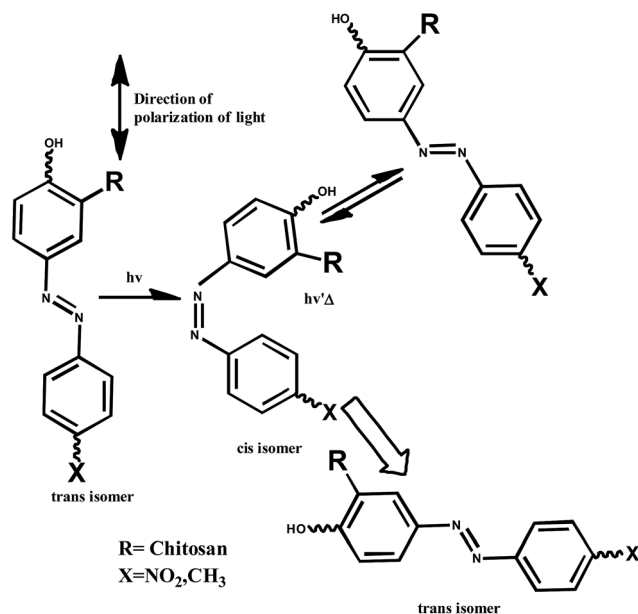


Fig. 7 Polarized light induced photoisomerization of chitosan attached azobenzene derivatives.

mobility and relaxation of the polymer backbone. Recently Kozanecka-Szmigiel *et al.* reported the photoinduced birefringence in azobenzene poly(esterimide) film at blue excitation wavelengths due to *trans-cis-trans* isomerization cycles associated with both the  $\pi-\pi^*$  and  $n-\pi^*$  transitions and the result is in good agreement with our investigation.<sup>18</sup>

The fitted dynamic parameters for both the derivatives are listed in Table 2. In sample CHNAB the value of  $k_a$  is less due to the presence of intermolecular hydrogen bonding in *cis* conformation, between nitro and hydroxyl group (Fig. 7) where as in case of CHMAB hydrogen bonding is absent. Hence rate of isomerisation is higher in CHMAB. Mobility rate  $k_b$  is same in both the derivative. Fast decay rate constant  $k_c$  is higher in case of CHNAB because *cis-trans* back-reaction starts more favourably in case of CHNAB due to intramolecular hydrogen bonding as compared to CHMAB. Slow rate constant  $k_d$  is higher in case of CHMAB as it needed more time to be in contact with the circular polarized light.

Long term stability of birefringence ( $E_n$ ) is more in case of CHNAB as compared with that of CHMAB. This is also shown in the Fig. 6, when the pump laser turned off, the decreased values of birefringence for sample CHNAB are much larger than that for sample CHMAB. The rigid aromatic structure of CHMAB limits the relaxation process of the oriented chromophore groups.

## Conclusions

Thermal study of azo derivatives established that CHMAB is thermally more stable than CHNAB. The Schiff base containing methyl group CHMAB, shows wide spectrum antimicrobial activity against *S. aureus* which is much higher compared to free chitosan. The results of the photoinduced birefringence showed

Table 2 Fitted dynamic parameters at room temperature for CHNAB and CHMAB

Parameters	Sample CHMAB	Sample CHNAB
$k_a$ ( $s^{-1}$ )	0.034	0.016
$k_b$ ( $s^{-1}$ )	0.004	0.004
$k_c$ ( $s^{-1}$ )	0.0103	0.034
$k_d$ ( $s^{-1}$ )	0.0025	0.023
$E_n$	0.76	0.64

that the long term stability of birefringence is more in case of derivative having nitro group. The studies indicate that the materials can be used as bio-optical devices for biomedical applications.

## References

- 1 Y. Cui, H. Ren, J. Yu, Z. Wang and G. Qian, *Dyes Pigm.*, 2009, **81**, 53–57.
- 2 F. Qiu, H. Xu, Y. Cao, Y. Jiang, Y. Zhou, J. Liu and X. Zhang, *Mater. Charact.*, 2007, **58**, 275–283.
- 3 V. Bruno, A. Castaldo, R. Centore, A. Sirigu, F. Sarcinelli, M. Casalbani and R. Pizzoferrato, *J. Polym. Sci., Part A: Polym. Chem.*, 2002, **40**, 1468–1475.
- 4 Y. Yang, Q. He, L. Duan, Y. Cui and J. Li, *Biomaterials*, 2007, **28**, 3083–3090.
- 5 H. Jiang, W. Su, S. Caracci, T. J. Bunning, T. Cooper and W. W. Adams, *J. Appl. Polym. Sci.*, 1996, **61**, 1163–1171.
- 6 P. K. Bhowmik, S. Kamatam, H. Han and A. K. Nedeltchev, *Polymer*, 2008, **49**, 1748–1760.
- 7 N. Nigam, S. Kumar, P. K. Dutta and T. Ghosh, *Bull. Mater. Sci.*, 2015, **38**, 1639–1643.
- 8 C. C. Teng, *Appl. Phys. Lett.*, 1992, **60**, 1538–1540.
- 9 M. A. Mortazavi, A. Knoesen, S. T. Kowel, R. A. Henry, J. M. Hoover and G. A. Linsay, *Appl. Phys. B*, 1991, **53**, 287–295.
- 10 K. D. Singer, M. G. Kuzyk, W. R. Holland, J. E. Sohn, S. L. Lalama, R. B. Comizzoli, H. E. Katz and M. L. Schilling, *Appl. Phys. Lett.*, 1988, **53**, 1800–1802.
- 11 D. G. Girton, S. L. Kwiatkowski, G. L. Lipscomb and R. S. Lytel, *Appl. Phys. Lett.*, 1991, **58**, 1730–1732.
- 12 I. Y. Kim, S. J. Seo, H. S. Moon, M. K. Yoo, I. Y. Park, B. C. Kim and C. S. Cho, *Biotechnol. Adv.*, 2008, **26**, 1–21.
- 13 D. Raafat and H. G. Sahl, *J. Microbiol. Biotechnol.*, 2009, **2**, 186–201.
- 14 S. Ghosh, A. K. Banthia and B. G. Maiya, *Org. Lett.*, 2002, **4**, 3603–3606.
- 15 D. R. Reddy and B. G. Maiya, *J. Phys. Chem. A*, 2003, **107**, 6326–6333.
- 16 A. K. Mahapatra, S. K. Manna and P. Sahoo, *Talanta*, 2011, **85**, 2673–2680.
- 17 S. Pei, X. Chen, Z. Jiang and W. Peng, *J. Appl. Polym. Sci.*, 2010, **117**, 2069–2074.
- 18 A. Kozanecka-Szmigiel, K. Switkowski, E. Schab-Balcerzak and D. Szmigiel, *Appl. Phys. B*, 2015, **119**, 227–231.
- 19 A. M. Musuc, D. Razus and D. Oancea, *Chimie, Anul XVI*, 2007, vol. 1, pp. 25–30.
- 20 F. Shahidi, J. K. V. Arachchi and Y. J. Jeon, *Trends Food Sci. Technol.*, 1999, **10**, 37–51.
- 21 S. Bian, J.-A. He, L. Li, J. Kumar and S. K. Tripathy, *Adv. Mater.*, 2000, **12**, 1202–1205.
- 22 T. Todorov, L. Nikolova and N. Tomova, *Appl. Opt.*, 1984, **23**, 4309–4312.
- 23 O. K. Song, C. H. Wang and M. A. Pauley, *Macromolecules*, 1997, **30**, 6913–6919.